Available online at www.sciencedirect.com
SCIENCE DIRECT®
PERGAMON
Polyhedron 22 (2003) 1845–1850
POLYHEDRON
www.elsevier.com/locate/poly

A poly(9,10-anthryleneethynylene)-based polyradical designed to be a ladder-like ferromagnetic spin coupling network

Takashi Kaneko *, Takahisa Makino, Hiroshi Miyaji, Akihisa Onuma, Masahiro Teraguchi, Toshiki Aoki

Department of Chemistry and Chemical Engineering, Faculty of Engineering, Niigata University, Ikarashi 2-8050, Niigata 950-2181, Japan

Received 6 October 2002; accepted 27 January 2003

Abstract

We synthesized monomers of poly(9,10-anthryleneethynylene)s which were anthracene derivatives substituted with one or two phenol residues at the β-position. The monomers were polymerized by Pd(0) catalyst to give the corresponding precursor polymer with $\bar{M}_n \approx 5 \times 10^3$. The polyradicals were synthesized by oxidation of the hydroxyl group. The magnetization plots of the polyradicals showed that the average ground state spin quantum number of the polyradical with two pendant phenoxyls in one anthracene unit ($S = 5/2$) became larger than that of the polyradical with one pendant phenoxyl ($S = 2/2$) at the same spin concentration (spin conc. ≈ 0.35 spin/phenoxyl unit). The statistical simulation of the ground spin states supported that this behavior was caused by ladder-like spin coupling network of the polyradical with two pendant phenoxyls in one anthracene unit.

Keywords: Conjugated polymer; Polyradical; Phenoxyl; Poly(aryleneethynylene); Anthracene; High-spin polymer

1. Introduction

Recently, there has been much attention to the polyradicals with a ladder-like ferromagnetic spin coupling network in the research field of π-conjugated polyradicals, whose progress is based on the synthesis of polyradicals with increasing values of the spin quantum number (S) in the electronic ground state [1–3]. The ladder-like spin coupling network possesses an advantage over 1D linear spin coupling system in that, even if the unpaired electrons are separated by one spin-defect, the strong magnetic interaction is maintained through another spin coupling pathway, while for the 1D linear spin coupling system the magnetic interaction between unpaired electrons separated by the spin-defect vanishes or weakens (Fig. 1).

Regioregular head-to-tail π-conjugated polymers possessing pendant radicals essentially have insensitivity to spin defects due to their connectivity in that the multiple spins are connected by one ferromagnetic coupler. However, it was nonavoidable that the exchange coupling constant (J_{ij}) between the unpaired electrons separated by the spin-defect decreases in response to the spacing unit due to the spin defect [3]. We have previously reported that the poly(9,10-anthryleneethynylene)-based polyradical (**1b**) with pendant phenoxyls at the β-position causes moderately strong ferromagnetic spin coupling ($2J = 39 \pm 3$ cm^{-1}) between neighboring units through the π-conjugated chain, but the average S value of **1b** was restricted due to the low spin concentration [4]. On the other hand, the average ground state spin quantum number of polyradical **2b** ($S = 5/2$), which has two pendant phenoxyls in one anthracene unit, became larger than that of **1b** ($S = 2/2$) at the same spin concentration [5]. In this study, we discussed the effect of the ladder-like spin coupling

* Corresponding author. Tel.: +81-25-262-6909; fax: +81-25-262-7010.
E-mail address: kanetaka@gs.niigata-u.ac.jp (T. Kaneko).

0277-5387/03/$ - see front matter
doi:10.1016/S0277-5387(03)00251-1

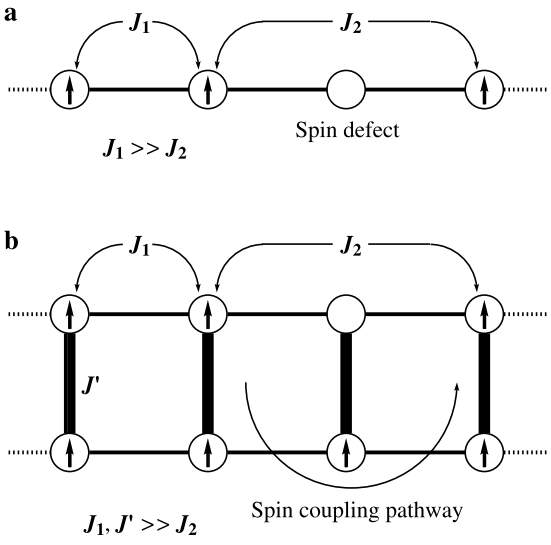

Fig. 1. Schematic illustration of (a) 1D spin coupling system and (b) ladder-like spin coupling network.

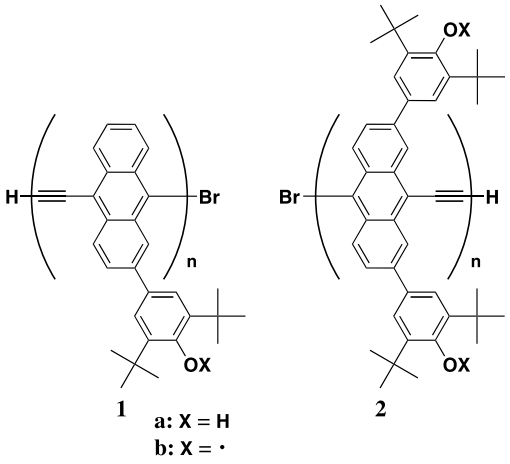

Chart 1.

network of **2b** compared with **1b** by using the statistical simulation of average S value (Chart 1).

2. Experimental

2.1. Materials

The monomers, 9-bromo-2-(3,5-di-*tert*-butyl-4-acetoxyphenyl)-10-(3-hydroxy-3-methyl-1-butynyl)anthracene [4] and 2,7-bis(4-acetoxy-3,5-di-*tert*-butylphenyl)-10-bromo-9-(3-hydroxy-3-methyl-1-butynyl)anthracene [5], were synthesized as previously described. Other conventional reagents were used as received or purified by conventional method.

2.2. Synthesis

Polymerization was carried out by the conditions described in Refs. [4,5]. The monomer (0.3 mmol), tetrakis(triphenylphosphine)palladium(0) (3.5 mg, 0.003 mmol), and copper iodide (0.57 mg, 0.003 mmol) were placed in an Schlenk tube under a nitrogen atmosphere. Freshly distilled toluene (3 ml) was transferred to the tube, and the monomers were dissolved with stirring. 5 M KOH methanol solution (0.3 ml) was added to the monomer solution, and the mixture was heated at 110 °C for 3 h. After cooling the mixture, the crude product was purified by reprecipitation from chloroform into hexane or methanol.

The obtained polymers were dissolved in THF (15 ml) under a nitrogen atmosphere. DMSO (45 ml) was added to the solution, then aqueous 2.5 M KOH (5 ml) was added to its suspension. The mixture was stirred at 50 °C for 12 h, cooled to room temperature (r.t.), and neutralized with aqueous 3 N HCl. The organic product was extracted with chloroform, washed with water, and dried over anhydrous sodium sulfate. The solvent was evaporated, and the crude product was purified by reprecipitation from chloroform into methanol.

The polyradicals were prepared by chemical oxidation of the corresponding hydroxyl precursors with PbO_2 under nitrogen in a glovebox as follows. A degassed toluene or 2-methyltetrahydrofuran solution of the hydroxyl precursor (0.5–10 mM per phenol unit) was treated with 0.1–10 equiv. of recently prepared PbO_2, and was vigorously stirred for 0.5–2 h. After filtration the solution was used for spectroscopic and magnetic measurement.

2.3. ESR spectroscopic measurement

Solutions for ESR experiments were prepared under nitrogen in a glovebox and placed in quartz tubes sealed with septa and Parafilm. ESR spectra were taken on a JEOL JES-2XG ESR spectrometer with 100 kHz field modulation in the X-band frequency region. Signal positions were calibrated against an external standard of Mn^{2+}/MgO ($g = 1.981$). The 77 K ESR spectra were measured for the 2-methyltetrahydrofuran-glass sample using a small Dewar flask containing the liquid nitrogen, which was inserted into the cavity of the spectrometer. The spin concentrations of each sample were determined by careful double integration of the ESR signal calibrated with that of the 2,2,6,6-tetramethyl-1-piperidinyloxy standard solution.

2.4. Magnetic measurement

The solution of polyradical immediately after oxidation was used to give the sample diluted with diamagnetic toluene or 2-methyltetrahydrofuran. The sample

solution was contained in a diamagnetic capsule. Magnetization was measured using a Quantum Design MPMS-7 SQUID magnetometer. The magnetization was measured from 0.5 to 7 T at 2 K. The static magnetic susceptibility was measured from 2 to 150 K in a field of 0.5 T. The mean-field correction parameter, θ, corresponding to small intermolecular (antiferro)magnetic interaction was determined from curve fitting using the product of molar magnetic susceptibility (χ_{mol}) and T vs T data. The spin concentrations of each sample were determined by analyzing the saturated magnetization at 2 K using a SQUID magnetometer.

The fraction (x_i) of the ground spin states (S_i) and a sum of Brillouin functions (B(S_i)) were statistically simulated in consideration of spin exchange coupling only between neighboring units as follows.

For **1b**:

$$x_i = \frac{2S_i \sum_{X_i=0}^{N} F_1(X_i,\ S_i) p^{X_i}(1-p)^{(N-X_i)}}{\sum_i 2S_i \sum_{X_i=0}^{N} F_1(X_i,\ S_i) p^{X_i}(1-p)^{(N-X_i)}} \quad (1)$$

For **2b**:

$$x_i = \frac{2S_i \sum_{X_i=0}^{2N} F_2(X_i,\ S_i) p^{X_i}(1-p)^{(2N-X_i)}}{\sum_i 2S_i \sum_{X_i=0}^{2N} F_2(X_i,\ S_i) p^{X_i}(1-p)^{(2N-X_i)}} \quad (2)$$

$$\frac{M}{M_S} = \sum_i x_i \mathrm{B}(S_i) \quad (3)$$

where $F_1(X_i, S_i)$ and $F_2(X_i, S_i)$ are the number of cases in which S_i appears in N-mer with X_i unpaired electrons for **1b** and **2b**, respectively, and p is spin concentration (spin/phenoxyl unit).

3. Results and discussion

3.1. Synthesis of polyradicals

We synthesized monomers, 9-bromo-2-(3,5-di-*tert*-butyl-4-acetoxyphenyl)-10-(3-hydroxy-3-methyl-1-butynyl)anthracene and 2,7-bis(4-acetoxy-3,5-di-*tert*-butylphenyl)-10-bromo-9-(3-hydroxy-3-methyl-1-butynyl)anthracene, which had ethynyl and bromo groups to be linked with head-to-tail bonds by self-condensation. The polymerization of these monomers were carried out in the presence of the Pd(0) complex catalyst and the appropriate base, combining the deprotection of the ethynyl group and the cross-coupling to the aromatic halide to circumvent an oxidative coupling side reaction to produce diyne linkages, and the corresponding polymers were obtained by precipitation from the polymerization mixtures into hexane or methanol. The obtained polymers were converted to the corresponding hydroxyl polymers **1a** and **2a** after complete elimination of the protecting acetyl group by treatment with alkaline solution followed by precipitation into methanol. The polymers were soluble in chloroform, tetrahydrofuran, and aromatic solvents, but insoluble in alcohols and aliphatic hydrocarbons. The number average molecular weight and molecular weight distribution of the polymers were measured as $\bar{M}_n = 4.8 \times 10^3$ and $\bar{M}_w/\bar{M}_n = 1.4$ for **1a**, and $\bar{M}_n = 4.8 \times 10^3$ and $\bar{M}_w/\bar{M}_n = 1.5$ for **2a**, respectively, using GPC calibrated relative to polystyrene standards. The degree of polymerization calculated from Br analysis ($\overline{DP}_n \approx 4$ for **1a**, and $\overline{DP}_n \approx 6$ for **2a**) did not conflict with the fact that the GPC using polystyrene standards tended to overestimate the average molecular weight of poly(aryleneethynylene)s [6]. The UV–Vis spectrum of **2a** showed an absorption maximum (λ_{max}) at 612 nm (tetrahydrofuran, $\varepsilon = 1.2 \times 10^4$ cm^{-1} M^{-1}). The λ_{max} of **2a** shifted to longer wavelength compared with the previously reported λ_{max} for poly(1,4-phenyleneethynylene)s (360–450 nm) and poly[(9,10-anthryleneethynylene)-alt-(1,4-phenyleneethynylene)]s (450–540 nm) [6], which suggests that the electronic structure of the planar and π-conjugated anthracene skeleton contributes to developing the π-conjugation system throughout the backbone (Scheme 1).

The polyradicals **1b** and **2b** were obtained by oxidizing the polymers **1a** and **2a**, respectively, by treatment of the polymer solution with fresh PbO_2. The spin concentration of the polyradicals reached *ca*. 0.5 spin/phenoxyl unit by selecting the oxidative conditions. The polyradicals were appropriately stable for maintaining the initial spin concentration under the ESR and SQUID measurement conditions, and the half-life of the polyradicals were *ca*. 15 h at r.t. in the solution.

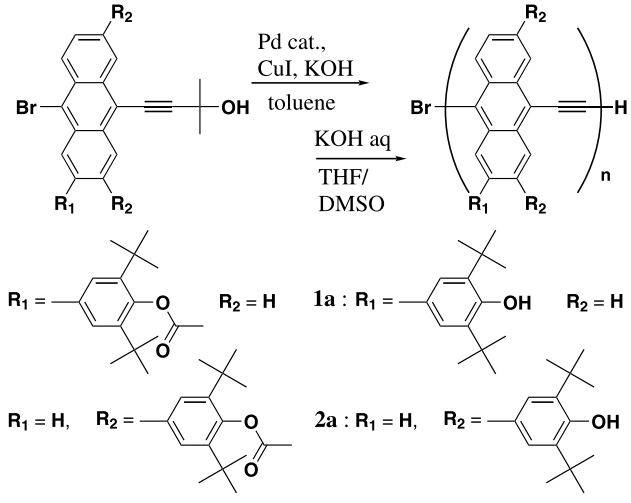

Scheme 1.

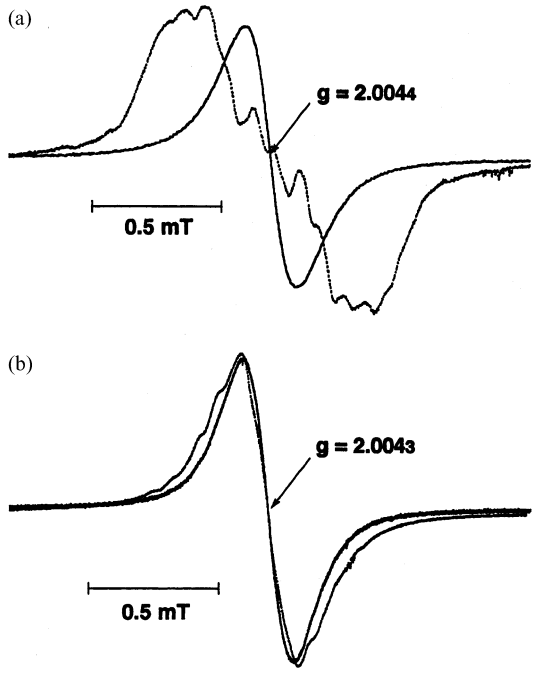

Fig. 2. ESR spectra of (a) **1b** (solid line: 0.5 mM, spin concentration = 0.40 spin/phenoxyl unit; dot line: 2.5 mM, spin concentration = 0.02 spin/phenoxyl unit in toluene), and (b) **2b** (solid line: 0.5 mM, spin concentration = 0.50 spin/phenoxyl unit in 2-methyltetrahydrofuran; dot line: 10 mM, spin concentration < 0.1 spin/phenoxyl unit in toluene) at r.t.

3.2. ESR spectra

The ESR spectra of **1b** and **2b** show unimodal broad signals at $g = 2.0043$–4 indicating the formation of the phenoxyl radical (Fig. 2). Broad hyperfine structures due to unresolved coupling of the protons of the phenoxyl ring and the anthracene skeleton appears at the lower spin concentration. On the other hand, well-resolved hyperfine structures were found for the corresponding monomeric radicals, and the hyperfine coupling constants estimated by the spectral simulation and the semiempirical calculation suggested the effectively delocalized spin density distribution over the anthracene unit in the polyradicals [4,5]. The $\Delta m_s = \pm 2$ forbidden transition ascribed to the triplet species is clearly observed at $g = 4$ in frozen toluene glass of **2b**, as well as **1b**, at 77 K, although no fine structure that gives zero-field splitting parameters D or E is detected at $g = 2$ because of the presence of several conformers and/or the long distance between unpaired electrons in the polyradical (Fig. 3).

3.3. Magnetic characterization

The magnetization of **1b** and **2b** were measured using a SQUID magnetometer. The sample was prepared as the frozen glass diluted in diamagnetic toluene or 2-methyltetrahydrofuran to minimize intermolecular in-

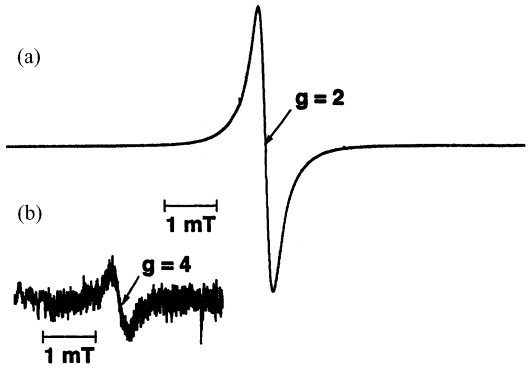

Fig. 3. ESR spectra of **2b** (10 mM, spin concentration = 0.50 spin/phenoxyl unit) in frozen 2-methyltetrahydrofuran glass at 77 K: (a) at $g = 2$ and (b) at $g = 4$.

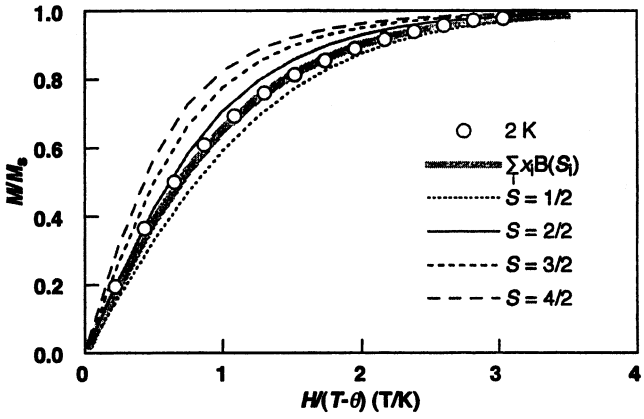

Fig. 4. Normalized plots of magnetization (M/M_s) vs the ratio of magnetic field and the effective temperature ($H/(T-\theta)$) for **1b** (spin concentration = 0.36 spin/phenoxyl unit) in frozen toluene glass (50 mM) at $T = 2$ K (○), and theoretical curves corresponding to $S = 1/2$, 1, 3/2, and 2 Brillouin functions, where θ is a weak antiferromagnetic term, and was determined to be -0.3 K from the $\chi_{mol}T$ vs T plots. Bold line: Statistical simulation curve for **1b** with 0.36 spin/phenoxyl unit and DP = 4.

teractions. The magnetization (M) normalized by saturated magnetization (M_s), M/M_s, of **1b** and **2b** are plotted versus the ratio of magnetic field (H) and the effective temperature ($T-\theta$), and compared with the theoretical Brillouin curves as shown in Figs. 4 and 5, respectively. In spite of the polyradicals of the same spin concentration (**1b**: 0.36, **2b**: 0.37 spin/phenoxyl unit), the plots of **2b** are located almost on the theoretical Brillouin curve of $S = 5/2$ at 2 K, while the plots of **1b** are located almost on the theoretical curve of $S = 2/2$.

Regioregular head-to-tail π-conjugated polymers possessing pendant radicals essentially have a ferromagnetic connectivity throughout the polymer chain irrespective of spin defects, because the multiple spins are connected by one ferromagnetic coupler. However, since the exchange coupling constant (J_{ij}) between the unpaired electrons decreases in response to the spacing unit, in consideration of spin exchange coupling only between

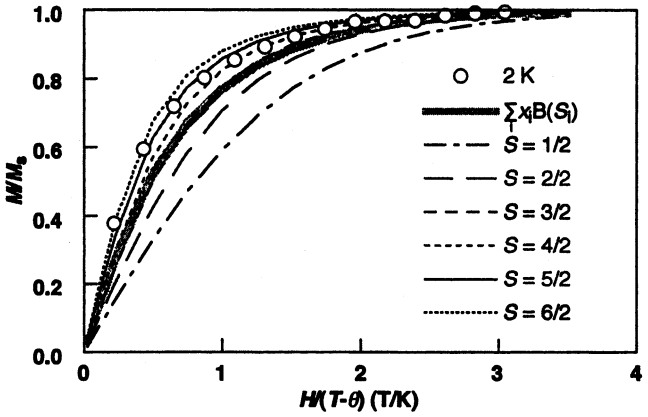

Fig. 5. Normalized plots of magnetization (M/M_s) vs the ratio of magnetic field and the effective temperature ($H/(T-\theta)$) for **2b** (spin concentration = 0.37 spin/phenoxyl unit) in frozen 2-methyltetrahydrofuran glass (10 mM) at $T = 2$ K (○), and theoretical curves corresponding to $S = 1/2$, 1, 3/2, 2, 5/2 and 3 Brillouin functions, where θ is a weak antiferromagnetic term, and was determined to be -0.3 K from the $\chi_{mol}T$ vs T plots. Bold line: Statistical simulation curve for **2b** with 0.37 spin/phenoxyl unit and DP = 6.

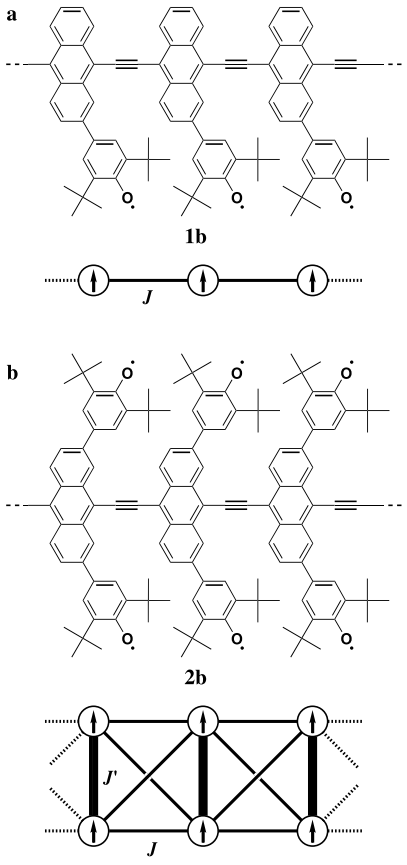

Fig. 6. Spin connectivity of (a) **1b** and (b) **2b** in consideration of spin exchange coupling only between neighboring units. J: moderately strong ferromagnetic coupling through the dianthrylacetylene unit; J': very strong ferromagnetic coupling through the anthracene unit.

neighboring units the connectivity of **1b** and **2b** can be shown as Fig. 6.

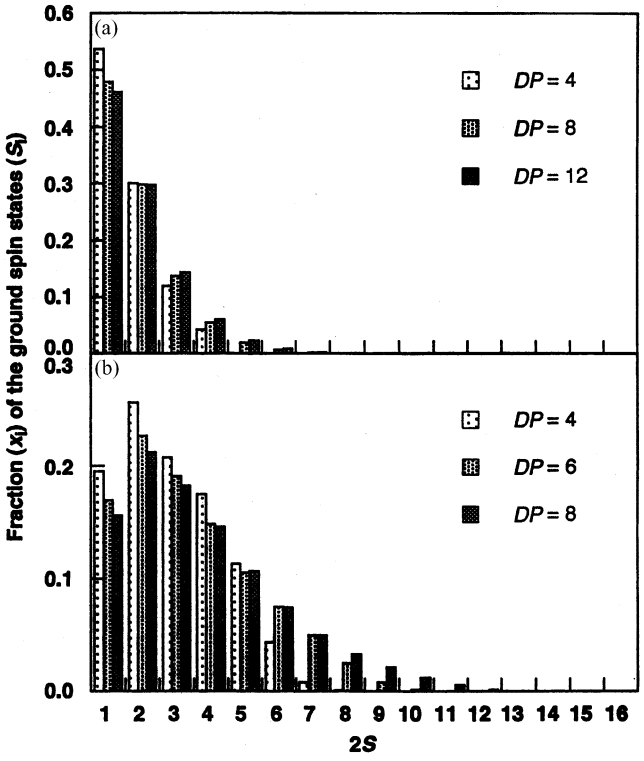

Fig. 7. Distribution of the ground spin states statistically simulated for the various oligomers (spin concentration = 0.35 spin/phenoxyl unit) of (a) **1b** and (b) **2b** in consideration of random and statistical spin defects.

The distribution of the generated radical along the main chains is random and statistical on the assumption that each pendant phenol group along the main chain has equivalent reactivity in the oxidation or radical generation process. In consideration of random and statistical spin defects, the distribution of the ground spin states is simulated for the various oligomers of **1b** and **2b**, and is shown in Fig. 7. In the spin concentration < 0.35 spin/phenoxyl unit, the distribution of the ground spin states is not affected by the chain length, but that of **2b** appears at the higher spin state than that of **1b**. This tendency is remarkable with spin concentration as shown in Fig. 8. Sums of Brillouin functions weighted with fractions (x_i) of the ground spin states (S_i) are simulated for **1b** with 0.36 spin/phenoxyl unit and DP = 4, and for **2b** with 0.37 spin/phenoxyl unit and DP = 6, and are shown in Figs. 4 and 5, respectively. The simulated curve of **2b** is almost agreed with the theoretical Brillouin curve of $S = 3/2$, and has the larger average S value than that of **1b** ($S = 1/2$–$2/2$) as well as the experimental plots. The experimental plots are located on or slightly upward from the simulated curves. This deviation from the simulated curves probably contains the contribution of the magnetic interaction between not neighboring units and/or the heterogeneous radical generation process.

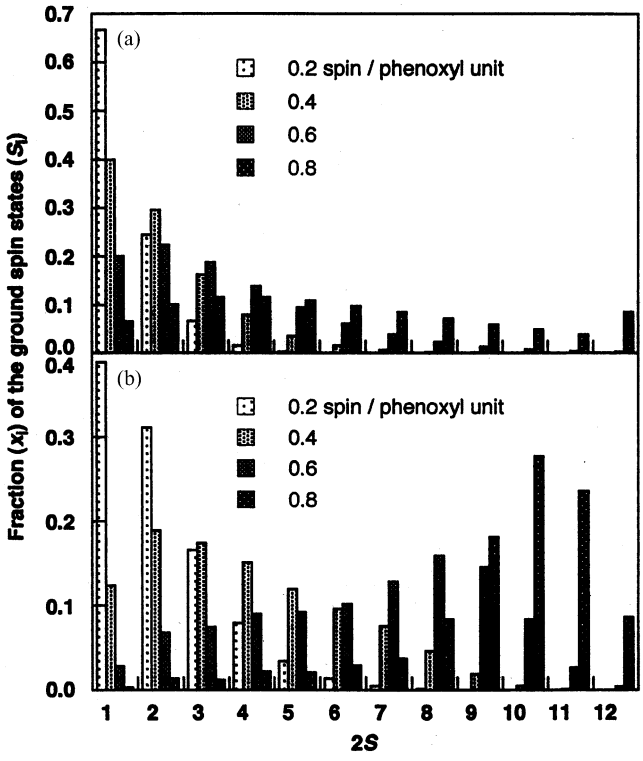

Fig. 8. Distribution of the ground spin states statistically simulated for (a) **1b** (DP = 12) and (b) **2b** (DP = 6) with various spin concentration in consideration of random and statistical spin defects.

4. Conclusions

The statistical simulation of the ground spin states supported that the average ground state spin quantum number of polyradical **2b** ($S = 5/2$) became larger than that of **1b** ($S = 2/2$) at the same spin concentration because **2b** consists of ladder-like spin coupling network. It was found that the 1D linear π-conjugated polyradical with the ladder-like spin coupling network was effective in increase of the apparent S value in the electronic ground state. The 1D linear π-conjugated polyradical with the ladder-like spin coupling network will be one of the possible candidates for magnetic polymer materials because the polymerization to produce linear polymers can be easy to access and can avoid the cross-linking that leads to the formation of insoluble polymer networks.

Acknowledgements

This work was partially supported by a Grant-in-Aid for encouragement of young scientists (No. 12750775), and for exploratory research (No. 14655344) from JSPS, by a grant for promotion of Niigata University Research Projects, and by Yazaki Memorial Foundation for Science and Technology. We thank for Prof. H. Nishide (Waseda University) for the use of their SQUID magnetometer.

References

[1] (a) D.A. Dougherty, Acc. Chem. Res. 24 (1991) 88;
(b) H. Iwamura, N. Koga, Acc. Chem. Res. 26 (1993) 346;
(c) A. Rajca, Chem. Rev. 94 (1994) 871;
(d) H. Nishide, Adv. Mater. 7 (1995) 937.
[2] (a) I. Fujita, Y. Teki, T. Takui, T. Kinoshita, K. Itoh, F. Miko, Y. Sawaki, H. Iwamura, A. Izuoka, T. Sugawara, J. Am. Chem. Soc. 112 (1990) 4074;
(b) D.A. Kaisaki, W. Chang, D.A. Dougherty, J. Am. Chem. Soc. 113 (1991) 2764;
(c) S. Sasaki, H. Iwamura, Chem. Lett. (1992) 1759;
(d) S. Utamapanya, H. Kakegawa, L. Bryant, A. Rajca, Chem. Mater. 5 (1993) 1053;
(e) A. Ito, K. Ota, K. Tanaka, T. Yamabe, K. Yoshizawa, Macromolecules 28 (1995) 5618;
(f) H. Oka, T. Tamura, Y. Miura, Y. Teki, Polym. J. 31 (1999) 979.
[3] (a) T. Kaneko, S. Toriu, Y. Kuzumaki, H. Nishide, E. Tsuchida, Chem. Lett. (1994) 2135;
(b) H. Nishide, T. Kaneko, T. Nii, K. Katoh, E. Tsuchida, K. Yamaguchi, J. Am. Chem. Soc. 117 (1995) 548;
(c) H. Nishide, T. Kaneko, S. Toriu, Y. Kuzumaki, E. Tsuchida, Bull. Chem. Soc. Jpn 69 (1996) 499;
(d) H. Nishide, T. Kaneko, T. Nii, K. Katoh, E. Tsuchida, P.M. Lahti, J. Am. Chem. Soc. 118 (1996) 9695;
(e) H. Nishide, T. Maeda, K. Oyaizu, E. Tsuchida, J. Org. Chem. 64 (1999) 7129;
(f) H. Nishide, M. Takahashi, J. Takashima, E. Tsuchida, Polym. J. 31 (1999) 1171;
(g) M. Miyasaka, T. Yamazaki, E. Tsuchida, H. Nishide, Macromolecules 33 (2000) 8211;
(h) P.J. van Meurs, R.A.J. Janssen, J. Org. Chem. 65 (2000) 5712.
[4] T. Kaneko, T. Matsubara, T. Aoki, Chem. Mater. 14 (2002) 3898.
[5] T. Kaneko, T. Makino, H. Miyaji, M. Teraguchi, T. Aoki, M. Miyasaka, H. Nishide, J. Am. Chem. Soc. 125 (2003) 3554.
[6] (a) U.H.F. Bunz, Chem. Rev. 100 (2000) 1605;
(b) R. Giesa, J. Macromol, Sci. Rev. Macromol. Chem. Phys., Sect. C 36 (1996) 631.